Effect of Preoxidation Temperature on the Reduction Kinetics of Ilmenite Concentrate

KYUNGSOB CHOI[1] and HYUNSIK PARK[2,3]

1.—Korea Institute of Geoscience and Mineral Resources (KIGAM), University of Science & Technology (UST), Daejeon 34132, South Korea. 2.—Resource Recovery Research Center, Mineral Resources Research Division, Korea Institute of Geoscience and Mineral Resources (KIGAM), Daejeon 34132, South Korea. 3.—e-mail: Hyunsik.park@kigam.re.kr

The preoxidation of ilmenite affects its reduction kinetics because of the change in the phases and morphologies, depending on the oxidation temperatures. To confirm the effect of the oxidation temperature on the reduction kinetics, we examined the reduction reaction of ilmenite samples oxidized at 873–1273 K in a H_2–50 vol.% CO atmosphere at a reduction temperature of 1273 K. The reduction rate of the ilmenite oxidized at low temperature (873–1073 K) was faster than that of the ilmenite oxidized at high temperature (1173–1273 K). This behavior was ascribed to pseudobrookite, formed by combination of the hematite and rutile at a high oxidation temperature. Ilmenite samples, respectively oxidized at 873 K and 1273 K, were selected to study the effects of the hydrogen partial pressure and reduction temperature on reduction kinetics. The reduction of the ilmenite sample oxidized at 873 K was controlled by nucleation and nuclei growth. However, the sample oxidized at 1273 K was controlled by the chemical reaction occurring during the reduction. As regards the subsequent smelting process, the ilmenite oxidized during the preoxidation process had the advantages of a high conversion degree and low energy consumption.

INTRODUCTION

Titanium minerals have become some of the most significant resources for advanced materials in industries because of technological development. Ilmenite is a natural mineral with an abundant reserve of titanium. Ilmenite with a TiO_2 content of less than 50 wt.% is upgraded to synthetic rutile or titanium slag at high temperatures to prevent the generation of a large amount of chemical waste from hydrometallurgical processes.[1,2] Pyrometallurgical processes, however, release large volumes of greenhouse gas, such as carbon dioxide, because coal or coke are used as the reducing agents. In recent years, as carbon dioxide emission regulations have become more stringent because of the global warming issue, numerous studies have been conducted on replacing conventional processes with methods that reduce greenhouse gas generation, such as using hydrogen.[1,3–8] Compared with conventional processes, ilmenite reduction, using hydrogen-containing gases, has the advantage of faster reduction rates.[1,9] Ilmenite is reduced by hydrogen through the solid–gas reaction between 1173 K and 1473 K, whereas the reduction temperatures of titania slag by carbon is over 1873 K.[10] The final products of hydrogen reduction are primarily metallic iron, TiO_2, and M_3O_5 solid solutions (M = Fe and Ti). Some researchers have examined ilmenite reduction using a mixture of H_2, CO, and CH_4 gases.[11–14] The kinetics of ilmenite reduction by hydrogen is controlled by diffusion models[10,15,16] or chemical reaction models.[3,5] The apparent activation energy for reaction varies from 50 kJ/mol to 170 kJ/mol, depending on the reduction conditions and kinetics mechanism.[17]

The preoxidation process introduced to improve the level of reduction has different phases and morphologies depending on the oxidation temperature.[18–20] Gupta et al.[21,22] and Zhang and

Ostrovski[20] have shown the formation of the intermediate phase of $Fe_2Ti_2O_7$ during heating in oxygen below 973 K. This compound was decomposed into hematite and rutile below 1073 K, whereas the intermediate phase was changed to pseudobrookite and hematite above 1073 K. In contrast, using ilmenite from the Panzhihua deposit (Sichuan province, China), Fu et al.[23] have reported that $Fe_2Ti_3O_9$ (crystallographic shear structure, not pseudorutile), rutile, and hematite were stable phases in an air atmosphere between 773 K and 1073 K. Morphological studies have been conducted on ilmenite oxidation to obtain visual information associated with the reaction mechanism.[24,25] Using scanning electron microscopy (SEM), Zhang et al.[24] have confirmed the variation in the surface and interior morphology of oxidized ilmenite along with the oxidation temperature. A hematite layer with a thickness of 1–2 μm, initially formed on a particle surface, was maintained, regardless of the oxidation time. Needle-like rutile grains were produced inside ilmenite particles under a temperature of 1073 K, and irregular rutile grains were scattered across the pseudobrookite matrix, formed by hematite and rutile combining. Accordingly, the oxidation process results in significantly different phases and particle morphologies depending on the temperature.[24] Previous preoxidation and reduction kinetics studies focused only on other reduction factors, such as the gas composition or particle characteristics. The oxidation temperature effect is sufficient to change the rate-controlling mechanism and kinetics in the subsequent reduction step.

Preoxidation is known to be effective in the titanium industry. There was a difference in morphology between the products generated by the different oxidation temperatures in the preoxidized ilmenite.[24] However, although oxidation temperature has a tremendous effect on the reduction kinetics, no research has been conducted. During the present study, we investigated the reduction of an oxidized domestic ilmenite concentrate by H_2 and CO gases to clarify the effect of the oxidation temperature on the reduction reaction. We conducted detailed analyses of the reduction mechanism of preoxidation ilmenite. The effects of partial pressure and temperature on the reduction were examined. The results were applied to various kinetic models and in the isoconversion method to obtain the activation energy. Finally, the conversion degree and energy consumption were investigated to confirm the advantages of the preoxidation process.

EXPERIMENTAL

Ilmenite concentrate obtained from domestic river sediments (Pyeongtaek, Korea) was used in our experiment. The particle sizes of the concentrate, obtained through wet magnetic separation, were less than 75 μm. Quantitative analysis was performed through x-ray fluorescence spectroscopy (S4 Explorer; Bruker AXS Inc., Madison, USA), and the ferric and ferrous ratios were determined through chemical titration analysis. The chemical composition of the concentrate is shown in supplementary Table S1. It was assumed that only oxygen in the iron oxides was removed during the reduction. All iron was regarded as ferric or ferrous iron; therefore, the maximum amount of oxygen that could be removed was 11.56%. The phases of the raw ilmenite concentrate were confirmed using x-ray diffraction (XRD; D/Max 2200; Rigaku, Tokyo, Japan, Cu-Kα, 40 kV voltage, 30 mA current). As shown in Fig. 1, the raw ilmenite concentrate comprised ilmenite ($FeTiO_3$), hematite (Fe_2O_3), and silica (SiO_2).

The raw ilmenite concentrate was heated in a muffle furnace to the desired temperature (873–1273 K) in an air atmosphere to obtain oxidized samples. When the temperature reached the target value, oxidation was conducted for 6 h. After oxidation, the samples were removed from the furnace and cooled to room temperature. As shown in supplementary Table S2, the isothermal reduction experiments on oxidized ilmenite were conducted using a customized thermogravimetric analyzer (TGA) in a H_2–CO atmosphere. The reduction behavior was investigated by measuring the change in the weight of the oxidized ilmenite during the reduction. In each experiment, the sample weight was limited to 1 g to prevent external effects, such as mass transfer and heat transfer. A fused silica crucible was filled with the sample and placed in the heating zone of the furnace. The furnace was purged with pure argon gas (99.999%) to create an inert atmosphere. When the furnace temperature reached the desired value, the H_2–CO mixture was injected into the furnace. The flow rate of the reduction gases was maintained at 200 mL/min, and the H_2:CO ratio was changed using a mass flow controller. The experimental temperature was
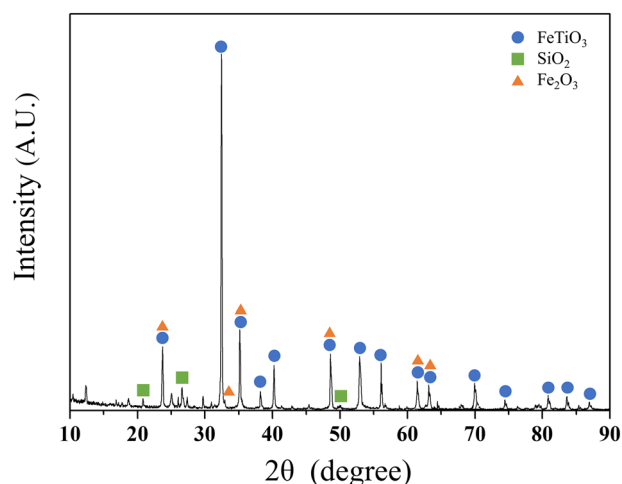

Fig. 1. XRD pattern of ilmenite concentrate obtained from Pyeongtaek, Korea.

controlled using a thermocouple with a proportional–integral–derivative system. The weight data were recorded by a microbalance of the TGA apparatus and saved on a computer every 3 s. The results were used to evaluate the reduction kinetics and activation energy. The phase and morphology of the samples were analyzed by employing XRD, SEM (JSM-6380LA; JEOL, Tokyo, Japan), and energy-dispersive x-ray analysis. The energy consumption was calculated using the thermodynamics program FactSage 8.0.

RESULTS AND DISCUSSION

The conversion degree of ilmenite during reduction is calculated by measuring the weight loss during the reaction using the following equation:

$$\alpha = \frac{m_0 - m_t}{m} \times 100 \qquad (1)$$

where α is the degree of conversion, m is the total removable oxygen present in the iron oxide of the ilmenite sample, m_0 is the initial weight of the sample before reduction, and m_t is the weight of the sample after reduction time t.

Effect of Oxidation Temperature on the Reduction Characteristics

Ilmenite was oxidized at 873–1273 K for 6 h in an air atmosphere to confirm the phase change dependence on the oxidation temperature. Figure 2 shows the XRD patterns of oxidized ilmenite. The phase transition behaviors differed considerably depending on the oxidation temperature. The main phases are Fe_2O_3 and TiO_2, with unreacted $FeTiO_3$ remaining at 873 K. This finding indicates that $FeTiO_3$ decomposes into Fe_2O_3 and TiO_2 during oxidation. The major phases of ilmenite oxidized at 973 K are Fe_2O_3 and TiO_2. At this temperature, $FeTiO_3$ completely disappears, and then $Fe_2Ti_3O_9$ (named H239) appears. Fu et al.[23] have also reported that $FeTiO_3$ changes to $Fe_2Ti_3O_9$ under oxygen-rich conditions at temperatures below 1073 K. As the oxidation temperature increases to 1073 K, new peaks of Fe_2TiO_5 combined with Fe_2O_3 and TiO_2 start to appear. The diffraction patterns of Fe_2O_3 and TiO_2 decreased slightly at 1073 K compared with the results at lower temperatures. Further, as the oxidation temperature increased to 1173 K and above, the intensity of the Fe_2TiO_5 peak increased significantly, while the Fe_2O_3 peak decreased. The XRD results indicated that the stable final products could be classified into two groups, namely Group 1, 873–1073 K, major phases of Fe_2O_3 and TiO_2; and Group 2, 1173–1273 K, major phases of Fe_2TiO_5 and TiO_2.

According to Zhang et al.,[24] the strong effect of the oxidized phase on the kinetics varies with the oxidation temperatures. As shown in Fig. 3, the reduction behaviors of the oxidized specimens were investigated at 1273 K to evaluate the influence of the oxidation temperature. The reduction behavior of oxidized ilmenites differed between Group 1 and Group 2 because of the phases of the oxidation products. Removable oxygen in oxidized ilmenite was generally enhanced as the oxidation temperature increased. In the temperature range of Group 1, the total weight loss increased along with oxidation temperature. However, the total weight loss of the oxidized ilmenites at temperatures exceeding 1173 K decreased with temperature because of pseudobrookite formation. The final weight loss of oxidized ilmenite at 1173 K was 0.13 g, i.e., similar to that at 1073 K. The reduction rate becomes sluggish after 1173 K, and when the oxidation temperature reaches 1273 K, the weight loss at the endpoint decreases to a low value similar to that at 973 K. The considerable decrease in the weight loss from 1173 K to 1273 K is related to the formation of Fe_2TiO_5. This finding indicates that pseudobrookite hindered the fast reduction of oxidized ilmenite particles.

Figure 4a and b show SEM images of oxidized ilmenite. The images were used to investigate the changes occurring in the morphology and the changes in oxidation temperature. The bright layer on the particle surface is Fe_2O_3, and the dark-gray color corresponds to the $FeTiO_3$ phase. Although the XRD patterns in Fig. 2 show the rutile phase formation between 873 K and 973 K, it is difficult to observe in the SEM images because rutile consists of nanometer-sized grains and mixes with hematite to form a network structure. Zhang et al.[24] conducted hydrochloric acid leaching and observed a rim structure with interconnected needle-like rutile grains. As shown in Fig. 4c, pseudobrookite (bright gray) forms close to the surface because of the combination reaction of the hematite and rutile present on the surface. Slightly darker and irregularly shaped rutile grains were observed in the pseudobrookite matrix. The morphology of ilmenite oxidized at 1173–1273 K differed significantly, as seen in Fig. 4d and e. The formation reaction of pseudobrookite occurred actively and occupied the entire interior of the particle. The rutile grains observed at 1073 K were larger in size, darker in color, and dispersed in the pseudobrookite matrix. The XRD and SEM results show that ilmenite decomposes into Fe_2O_3 and TiO_2 from 873 K to 1073 K. Numerous cracks form that increase the surface area, as well as reactive nuclei. As a result, the reduction rate increased when the oxidation temperature increased from 873 K to 1073 K. Further, when the oxidation temperature reaches 1173 K or higher, Fe_2O_3 and TiO_2 react and generate Fe_2TiO_5 with dense structures. Thermal effects occur because a higher temperature narrows the gas channel in the oxidized ilmenite and prevents the inflow of reducing gases. Accordingly, the reduction rate of oxidized ilmenite from 1173 K to 1273 K decreases significantly because of the formation of
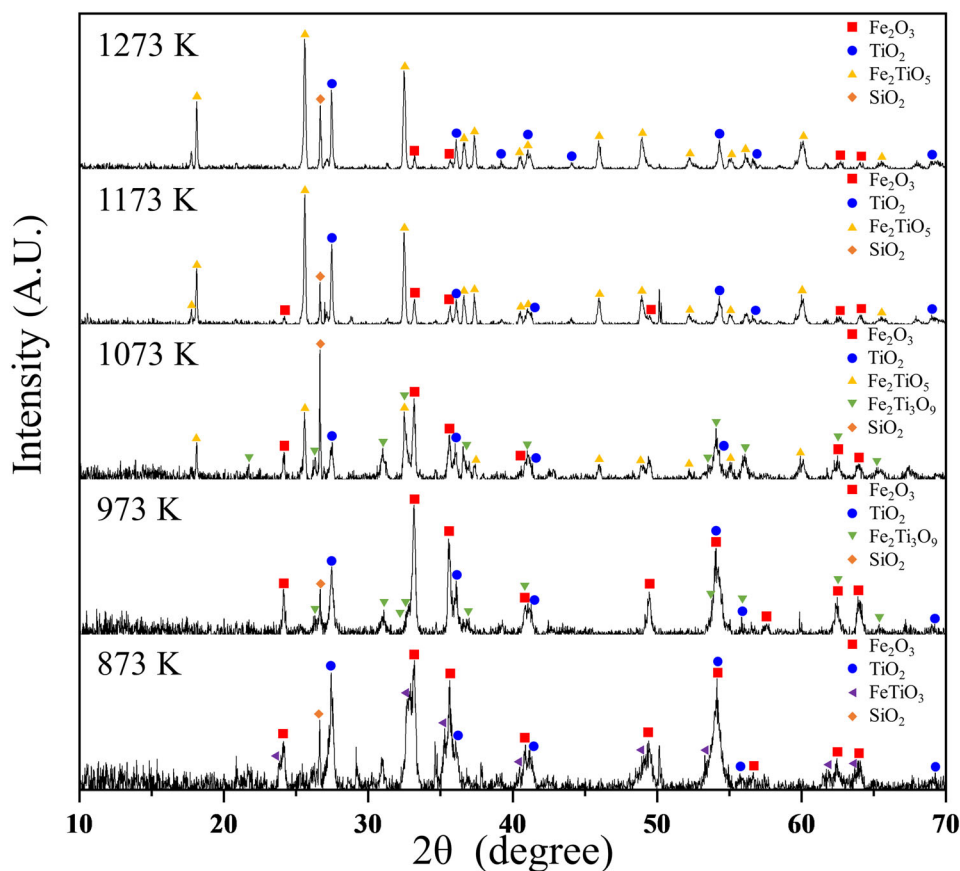
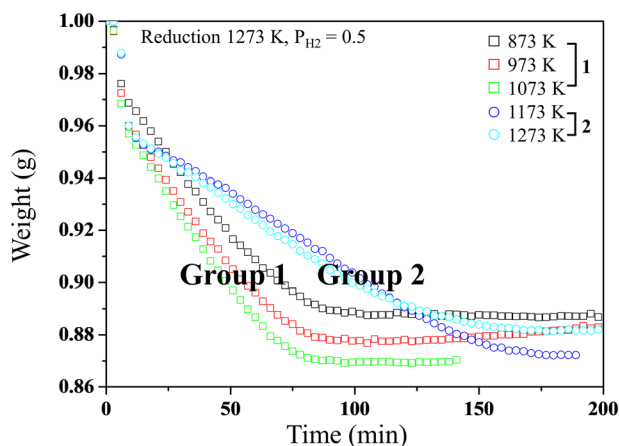Fig. 2. XRD patterns of ilmenite oxidized at 873–1273 K in air for 6 h.

Fig. 3. Change in weight of ilmenite oxidized at different temperatures during reduction in H_2–50 vol.% CO atmosphere at 1273 K.

Fe_2TiO_5. The oxidation temperature, therefore, determines the reduction kinetics.

Reduction Mechanism of Ilmenites Oxidized at Different Temperatures

Specimens oxidized at 873 K and 1273 K were selected for reduction to investigate the influence of the oxidation temperature on the reduction mechanism. In Fig. 5, the XRD results show that the ilmenites oxidized at 873 K and 1273 K were reduced at 1273 K for 0 min, 5 min, and 1 h under $P_{H2} = 0.5$ atm. As shown in Fig. 5a, the intensity of the peaks from ilmenite increased significantly while hematite decreased. This finding means that the ferric ion of hematite quickly changes into the ferrous ion of ilmenite. In addition, the intensity of the rutile peaks decreases considerably, indicating that the rutile participates with hematite in the reduction reaction of ferric ions into ferrous ions that form ilmenite. After 1 h, the peak of Fe was observed because the ferrous ion changed to metallic iron during the metallization reaction of ilmenite. The reduction of ilmenite oxidized at a high temperature can be seen in Fig. 5b. The initial pseudobrookite is reduced to ilmenite after 5 min, and metallic iron is generated after 1 h. The XRD results indicate that the reduction paths of oxidized ilmenite at different temperatures were the same. The oxidized ilmenites have different initial phases of hematite and pseudobrookite because of the difference in oxidation temperature. However, they combined with rutile to form ilmenite, and are subsequently reduced to produce iron. The reduction reactions according to the oxidation temperature are shown in Eqs. 2–5.[20,24]
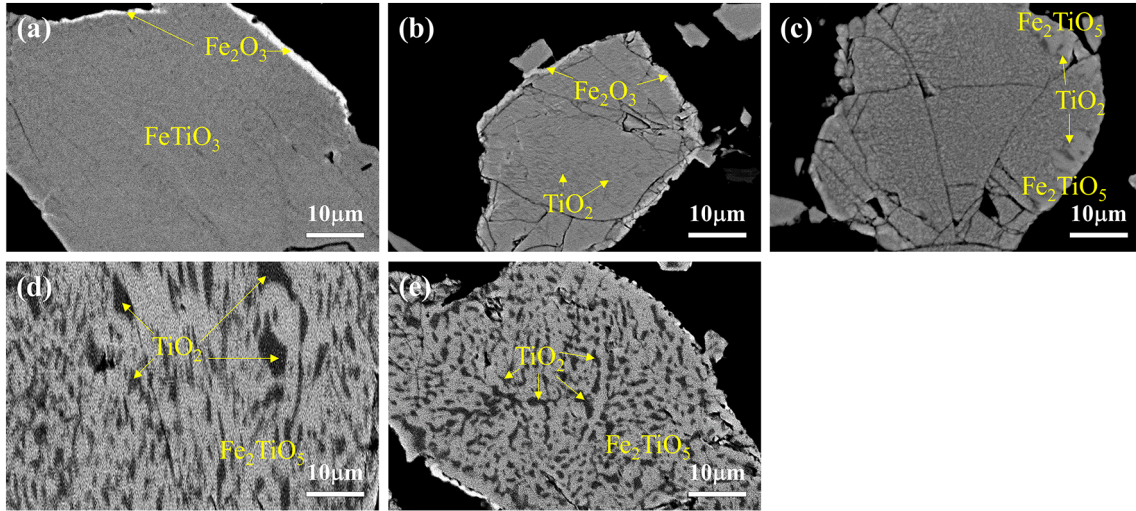
Low oxidation temperature

Fig. 4. SEM images of ilmenite oxidized in air for 6 h at (a) 873 K, (b) 973 K, (c) 1073 K, (d) 1173 K, and (e) 1273 K.
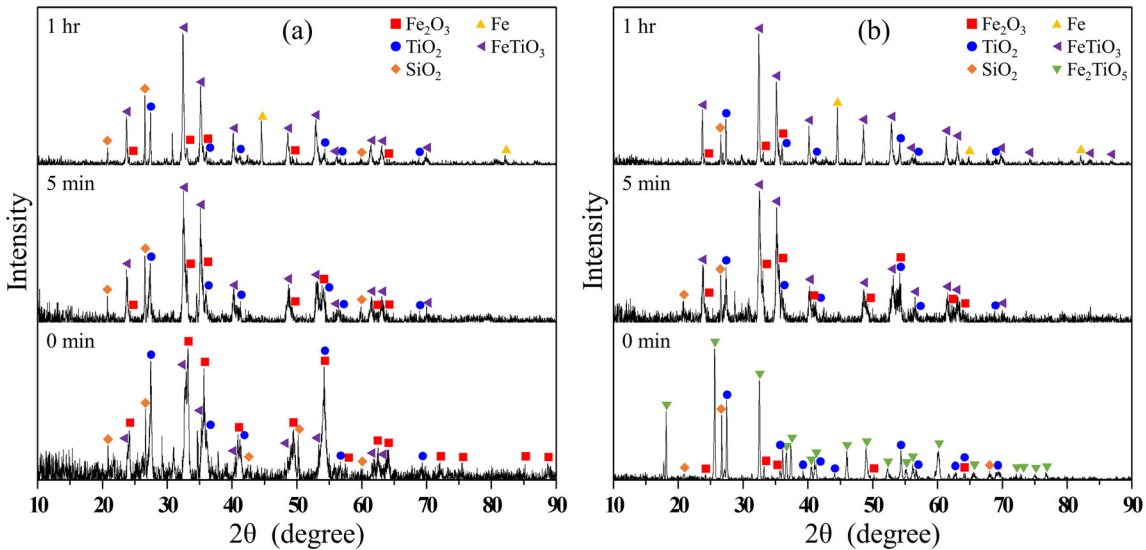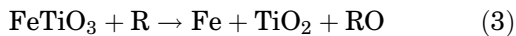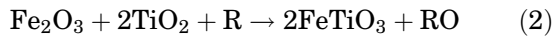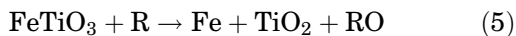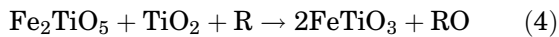

Fig. 5. XRD patterns of preoxidized ilmenite [(a) 873 K and (b) 1273 K] reduced at 1273 K for 0 min, 5 min, and 1 h under H_2–50 vol.% CO atmosphere.

$$Fe_2O_3 + 2TiO_2 + R \rightarrow 2FeTiO_3 + RO \qquad (2)$$

$$FeTiO_3 + R \rightarrow Fe + TiO_2 + RO \qquad (3)$$

High oxidation temperature

$$Fe_2TiO_5 + TiO_2 + R \rightarrow 2FeTiO_3 + RO \qquad (4)$$

$$FeTiO_3 + R \rightarrow Fe + TiO_2 + RO \qquad (5)$$

where R is the H_2 and CO. Figure 3 and the reduction reaction above show that the fast weight loss for 10 min corresponds to the ilmenite formation reaction and the subsequent slow weight loss is a reaction wherein the formed ilmenite is reduced to metallic iron.

To confirm the difference in the kinetic reaction according to the oxidation temperature, ilmenites oxidized at 873 K and 1273 K were reduced at 1273 K for 1 h, as shown by the SEM images in Fig. 6. The bright color is iron, the gray is ilmenite, and the dark-gray is the rutile phase. Figure 6a and b show that the ilmenite formed during the first reduction step was reduced to generate iron and rutile. However, it should be noted that there is a significant difference in the morphology of the iron. As shown in Fig. 4, cracks and pores formed in ilmenite oxidized at 873 K. The reducing gases flowing through these cracks reacted with the nuclei in the particle interior. As a result, iron particles occurred inside the particle. Meanwhile, in ilmenite oxidized at 1273 K, the reducing gases could not initially permeate inside the particles and instead reacted at the particle boundaries because

pseudobrookite, which has a dense structure, formed at 1273 K. Although the reduction reactions of ilmenites oxidized at different temperatures follow the same reduction path, the reaction rate is affected because of the morphological difference between hematite and pseudobrookite.

Effect of Hydrogen Partial Pressure

The samples were reduced at 1273 K at a $H_2/(H_2 + CO)$ ratio of 0.1–0.5 to investigate the influence of hydrogen partial pressure. The effect of the hydrogen partial pressure on the conversion degree is shown in Fig. 7. The overall reduction reaction by hydrogen was classified into two steps. The conversion degree rapidly reaches 0.3 in the first step and gradually increases after 10 min for all conditions. This finding indicates that the reaction rate in the first step was marginally affected by oxidation temperature and hydrogen partial pressure. In the second step, the effects of the hydrogen partial pressure and oxidation temperature become evident. The conversion degree of the sample oxidized at 873 K was 0.6 after 90 min of reduction at $P_{H2} = 0.1$ atm, whereas the conversion degree increased to 0.8 and 0.9 at $P_{H2} = 0.3$ and 0.5 atm, respectively. Regarding the sample oxidized at 1273 K, the conversion degree increased with the hydrogen partial pressure; however, it was

significantly lower than the sample oxidized at 873 K. The conversion degree after 90 min is 0.4, 0.5, and 0.7 at hydrogen partial pressures of 0.1, 0.3, and 0.5, respectively. Conclusively, the conversion degree is lower for samples of high temperature oxidation, agreeing with the results discussed in Section A. The reduction rate of oxidized ilmenite increases as the $H_2/(H_2 + CO)$ ratio increases, as shown in Fig. 7.

Effect of Reduction Temperature, and Kinetics Model Prediction

As shown in Fig. 8, Eq. 1 is used to obtain the conversion degrees during reduction at $P_{H2} = 0.5$ atm and 1173–1373 K for samples oxidized at 873 K and 1273 K. In the second step, the overall conversion degree for samples oxidized at 873 K was higher than at 1273 K. The reduction reaction is affected strongly by the oxidation and reduction temperatures. The reduction rate tends to be higher for samples oxidized at a lower temperature. The reduction rate rapidly increases along with the temperature for samples oxidized at higher temperatures.

The overall reduction reaction of oxidized ilmenite comprises a fast reaction in the first step and a slow reaction in the second step. Therefore, the reduction kinetics of preoxidized ilmenite was determined in
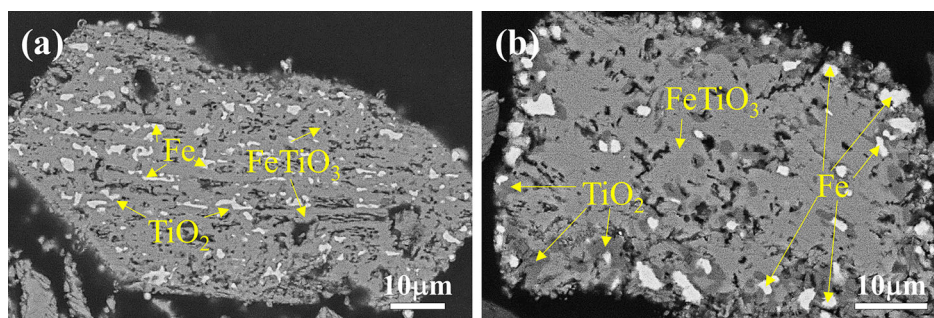

Fig. 6. SEM images of preoxidized ilmenite [(a) 873 K and (b) 1273 K] reduced at 1273 K for 1 h under H_2–50 vol.% CO atmosphere.
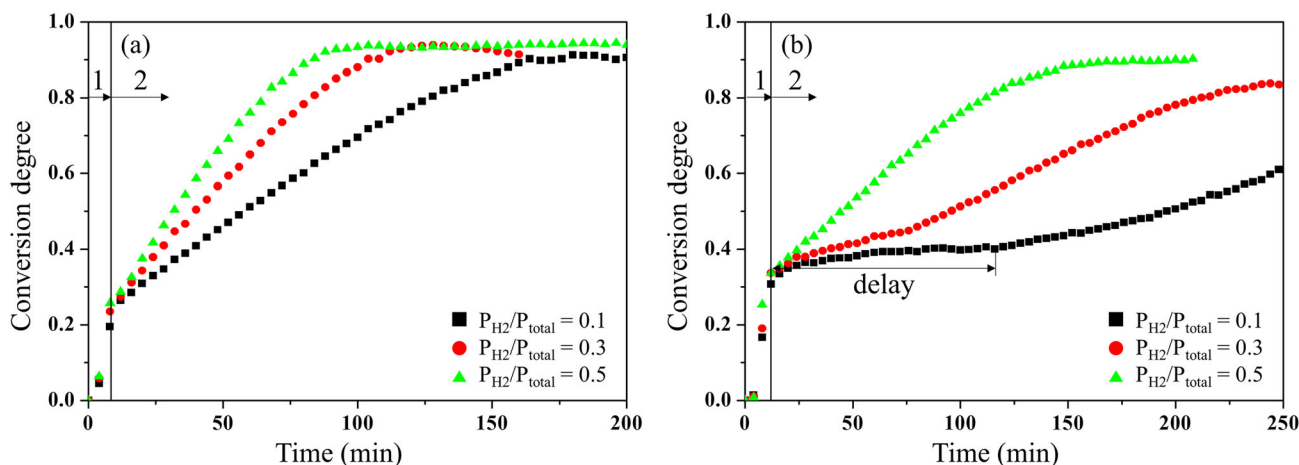

Fig. 7. Conversion degree of ilmenite oxidized at (a) 873 K and (b) 1273 K during reduction at different hydrogen partial pressures.
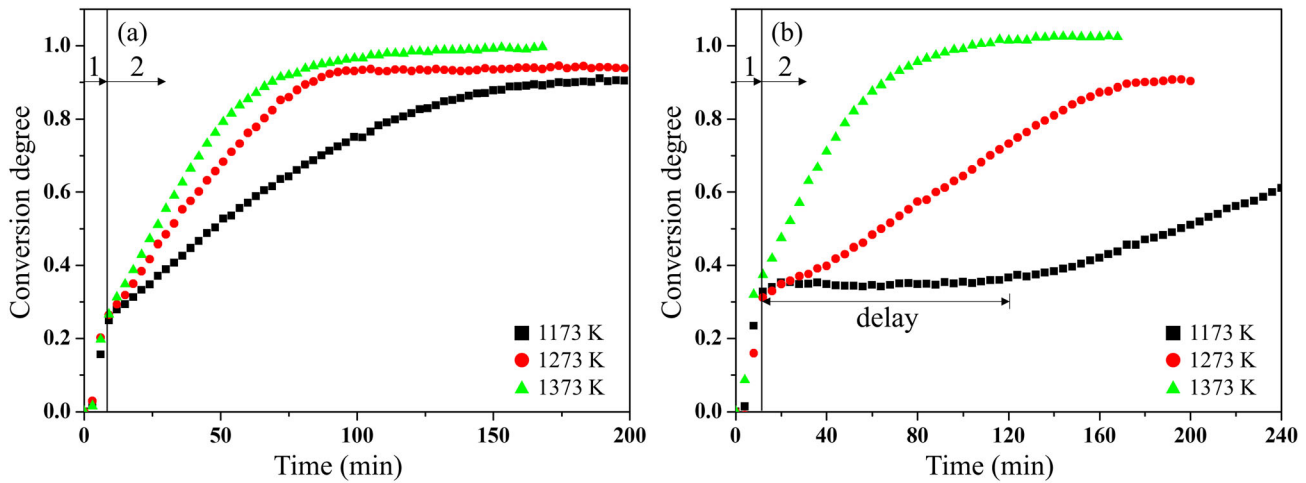
Fig. 8. Conversion degree of ilmenite oxidized at (a) 873 K and (b) 1273 K during reduction at different temperatures and P_{H2} = 0.5 atm.

the second step to clarify the effect of preoxidation. The reduction rate can be expressed generally as a function of reaction temperature T and conversion degree α, as follows:

$$\frac{d\alpha}{dt} = k(T) \cdot f(\alpha) \qquad (6)$$

where t is time, $k(T)$ is the rate constant, and $f(\alpha)$ is a function of the conversion degree by the kinetic reaction model. Equation 6 is rewritten as a function associated with the mechanism of the reaction process.

$$G(\alpha) = \int_0^\alpha \frac{d\alpha}{f(\alpha)} = \int_0^t k(T) \cdot d(t) = k(T) \cdot t \qquad (7)$$

Supplementary Table S3 shows the typical reaction model equations for $G(\alpha)$.[17,26,27] The experimental data of the conversion degree were applied to various kinetic equations to determine a suitable model, and the kinetic model was selected in which the plot of $G(\alpha)$ versus time showed a good linear relation.

As shown in Fig. 9a, the kinetic model for the reduction of ilmenite oxidized at 873 K is a power law, indicating that the reaction is controlled by nucleation and nuclei growth. Figure 9b shows that the reduction of ilmenite oxidized at 1273 K is controlled by the chemical reaction. This difference in the reduction mechanism according to the oxidation temperature is attributed to morphological changes. In the early stages of the oxidation process, ilmenite decomposes into hematite and rutile, resulting in numerous cracks and pores. Afterwards, the reducing gases are introduced into the particle interior through the gas channels, and nucleation and growth reactions occur. As the oxidation temperature increases, hematite and rutile are recombined, and broken particles aggregate to form a dense structure. As a result, the reducing gases cannot permeate inside the

combined particles, and a chemical reaction is restricted to the surface. It could be confirmed that these kinetic reaction models agree with the SEM images in Fig. 6. The slope, $k(T)$, of the graph in Fig. 9 is obtained using linear regression analysis. The activation energy is calculated using the Arrhenius equation, as follows:

$$k(T) = A \cdot \exp\left(-\frac{E}{RT}\right) \qquad (8)$$

where A is the pre-exponential factor, E is the activation energy, and R is the ideal gas constant. The value of E calculated for the reduction of ilmenite oxidized at 873 K is 55.79 kJ/mol and is 117.41 kJ/mol at 1273 K. These results indicate that the energy barrier of the reduction reaction for samples oxidized at 873 K is lower than that for samples oxidized at 1273 K. The overall reduction rate for specimens with a lower oxidation temperature is higher than specimens with a higher oxidation temperature.

Estimation of Activation Energy by Isoconversion Method

A predefined model that agreed with the experimental data was used for the kinetics analysis described above. This analysis involved the implicit assumption that the activation energy did not change during the entire reaction. The isoconversion method can calculate the activation energy at different values of α without a specific model equation.[17,26] Therefore, the method was employed to evaluate the activation energy without a kinetic law and compare it with the values obtained using the model fitting method. Equation 7 is rewritten as Eq. 9, as follows:

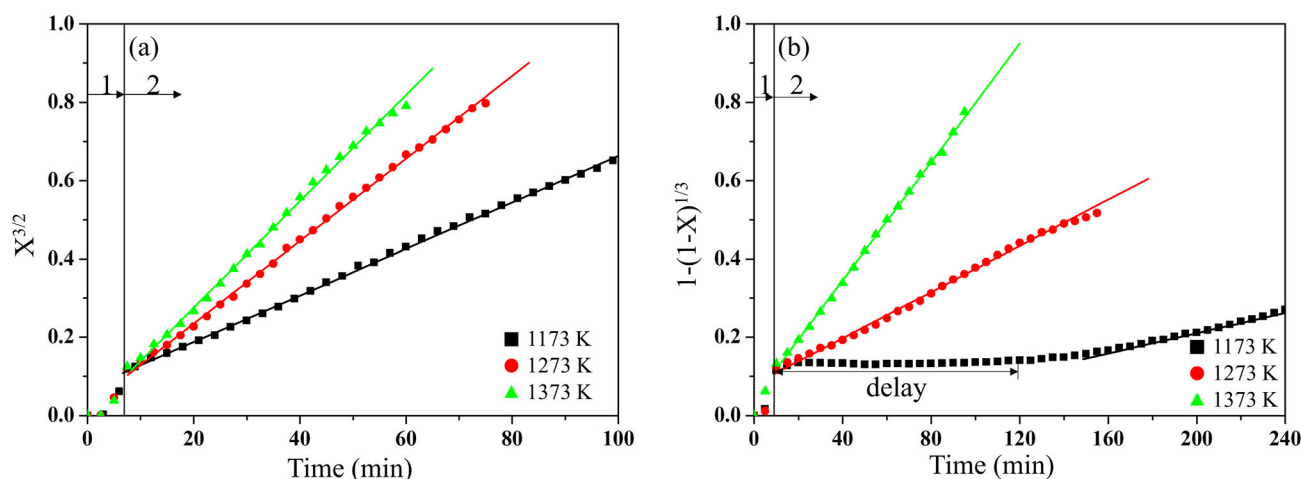$$\ln t_\alpha = \frac{E}{RT} + \ln\frac{G(\alpha)}{A} \qquad (9)$$

Fig. 9. (a) $X^{3/2}$ versus time for ilmenite oxidized at 873 K, and (b) $1 - (1 - X)^{1/3}$ versus time for ilmenite oxidized at 1273 K during reduction at 1173–1373 K in a H_2–CO atmosphere ($P_{H2} = 0.5$ atm).
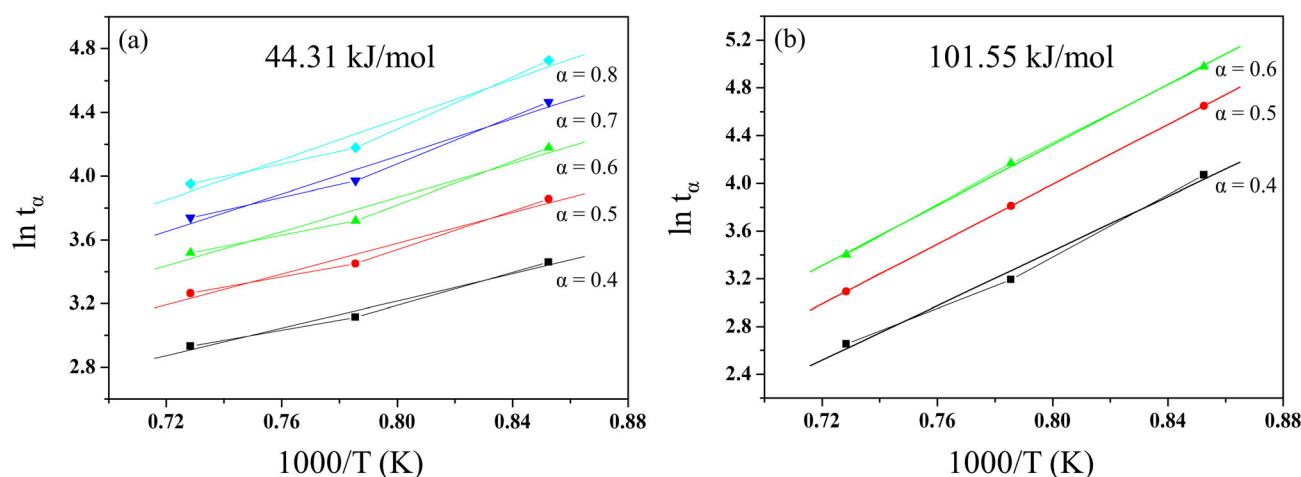

Fig. 10. In t_α versus $1/T$ for ilmenite oxidized at (a) 873 K and (b) 1273 K to estimate the activation energy using the isoconversion method.

where t_α is the time required to reach a fixed value of α. $G(\alpha)$ is constant because of the fixed value of α. The activation energy is calculated from the slope of the graph of In t_α versus $1/T$. The value of t_α corresponding to a given conversion degree was measured for each temperature. As shown in Fig. 10, the activation energy for the reduction of samples oxidized at 873 K is 44.31 kJ/mol, and the activation energy for the samples oxidized at 1273 K is 101.55 kJ/mol. The activation energy varies only slightly over the entire range of the conversion degree in the second step. These values are similar to those obtained using the model fitting method. This result confirms that the reduction of samples oxidized at 873 K is controlled by nucleation and nuclei growth, whereas that of samples oxidized at 1273 K is controlled by chemical reaction.

Advantages of the Preoxidation Process

Figure 11 shows the conversion degree for samples reduced at 1273 K in a H_2–50 vol.% CO

atmosphere. Raw ilmenite and preoxidized ilmenites show completely different conversion degrees. The reduction rate of ilmenites oxidized at 873 K occurs much faster than raw ilmenite during 5 min. The final conversion degree reached 0.935. In contrast, raw ilmenite reached a conversion degree of 0.757. The conversion degrees of oxidized ilmenites were greater than those of raw ilmenite during the entire time of reduction. This result shows that the preoxidation process improves the reduction behavior of raw ilmenite.

The energy consumption for the smelting process was calculated employing thermodynamic software, FactSage 8.0, to clarify the advantages of the preoxidation process. From the results shown in Fig. 11, the conversion degrees at 150 min were applied as the feed information for the smelting process, with the values being 75.7% and 95.3%, respectively. For the convenience of calculation, the initial ilmenite was assumed to be pure $FeTiO_3$, with an amount of 1 tonne. In Fig. 12a, the reduced ilmenite comprises 243.00 kg ilmenite, 390.24 kg

rutile, and 283.71 kg iron, corresponding to 75.7% of the conversion degree. In the process of preoxidation, the composition of the reduced ilmenite was 65.00 kg ilmenite, 489.77 kg rutile, and 345.53 kg iron. A general smelting operation temperature of 1948 K (1675°C) for ilmenite was set. In both instances, the amount of carbon was calculated when the TiO_2 content in the slag was at its maximum without forming pseudobrookite. These values were 35.34 kg and 22.90 kg, respectively. According to the calculated thermodynamic results after smelting, titania slag and liquid iron were produced in both processes, with their composition and production being the same, as shown in Fig. 12a and b. However, a considerable difference is shown between the two processes in terms of

Fig. 11. Conversion degrees of raw and oxidized ilmenite (873 K) reduced at P_{H2} = 0.5 atm and 1273 K.

energy consumption and the amounts of emission gases produced. After reducing raw ilmenite, the smelting process consumed 487 kWh per tonne, and the amount of emission gas was 80.88 kg per tonne; however, adding the preoxidation process reduces the energy consumption and emission gases by 61 kWh and 29.11 kg, respectively. This finding indicates that the preoxidation process reduces CO_2 emission gases related to global warming and the energy consumption in smelting.

CONCLUSION

We investigated the reduction kinetics of preoxidized ilmenite under a H_2–CO atmosphere. Ilmenite samples oxidized at 873–1273 K were reduced at 1273 K through hydrogen and carbon monoxide gases. The reduction rate was influenced strongly by the oxidation temperature, increasing along with the increase in oxidation temperature between 873 K and 1073 K. However, the reduction rate started to decrease above a temperature of 1173 K. This was because hematite and rutile, which were initially produced by oxidation, recombined to form pseudobrookite. The formation of pseudobrookite above 1173 K lowered the reaction kinetics because of its dense structure. The reduction reaction for both samples occurred in two steps, with the overall reaction kinetics being controlled by the reaction in the second step. The reduction rate of preoxidized ilmenite increased with the hydrogen partial pressure and reduction temperature. According to the model fitting method, the reduction of the ilmenite sample oxidized at 873 K was controlled by nucleation and nuclei growth, with the activation energy being 55.79 kJ/mol. The reduction of the ilmenite sample oxidized at 1273 K was controlled via chemical reaction, with the activation energy being
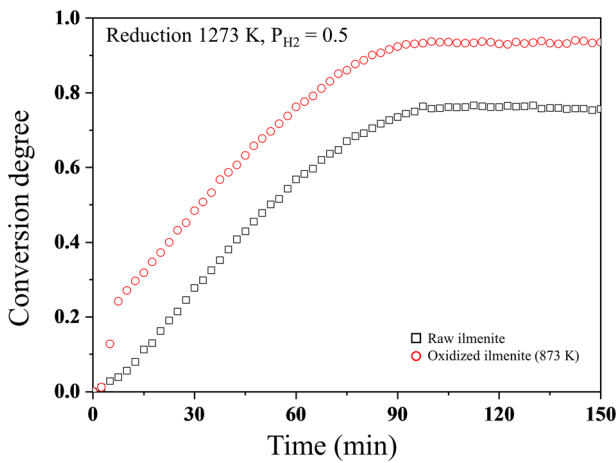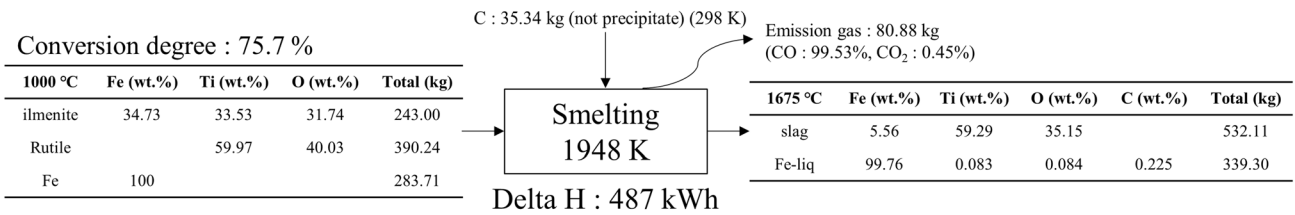
(a) Reduction – Smelting process

Conversion degree : 75.7 %

1000 °C	Fe (wt.%)	Ti (wt.%)	O (wt.%)	Total (kg)
ilmenite	34.73	33.53	31.74	243.00
Rutile		59.97	40.03	390.24
Fe	100			283.71

C : 35.34 kg (not precipitate) (298 K)

Smelting 1948 K

Delta H : 487 kWh

Emission gas : 80.88 kg
(CO : 99.53%, CO_2 : 0.45%)

1675 °C	Fe (wt.%)	Ti (wt.%)	O (wt.%)	C (wt.%)	Total (kg)
slag	5.56	59.29	35.15		532.11
Fe-liq	99.76	0.083	0.084	0.225	339.30

(b) Oxidation – Reduction – Smelting process

Conversion degree : 93.5 %

1000 °C	Fe (wt.%)	Ti (wt.%)	O (wt.%)	Total (kg)
ilmenite	34.73	33.53	31.74	65.00
Rutile		59.97	40.03	489.77
Fe	100			345.53

C : 22.90 kg (not precipitate) (298 K)

Smelting 1948 K

Delta H : 426 kWh

Emission gas : 51.77 kg
(CO : 99.53%, CO_2 : 0.45%)

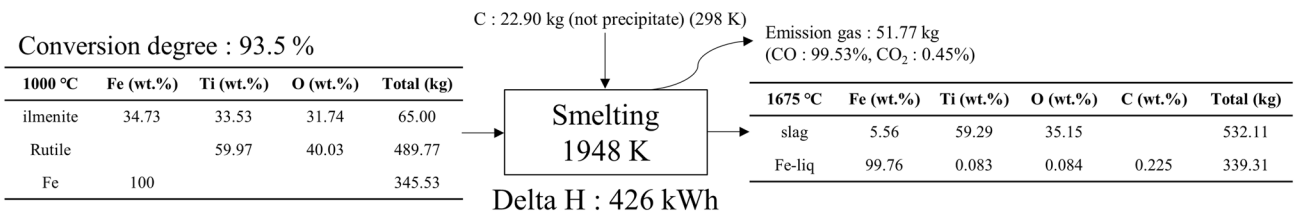| 1675 °C	Fe (wt.%)	Ti (wt.%)	O (wt.%)	C (wt.%)	Total (kg)
slag	5.56	59.29	35.15		532.11
Fe-liq	99.76	0.083	0.084	0.225	339.31

Fig. 12. Energy consumption of smelting process using different processes, namely (a) reduction–smelting process, (b) oxidation–reduction–smelting process.

117.41 kJ/mol. The isoconversion method was applied to the experimental data for both oxidation temperatures. The activation energies calculated using this method were 44.31 and 101.55 kJ/mol for oxidation temperatures of 873 K and 1273 K, respectively. Preoxidation considerably improved the reduction kinetics of raw ilmenite, and it was more effective at a temperature below 1073 K. During the smelting process, the addition of preoxidation decreased energy consumption and CO_2 emissions. Therefore, in smelting, adding the preoxidation process is effective for global warming.

ACKNOWLEDGEMENTS

CONFLICT OF INTEREST

The authors declare that they have no conflict of interest.

SUPPLEMENTARY INFORMATION

The online version contains supplementary material available at https://doi.org/10.1007/s11837-022-05480-0.

REFERENCES

1. W. Lv, X. Lv, J. Xiang, K. Hu, S. Zhao, J. Dang, K. Han, and B. Song, *Int. J. Hydrogen Energy* 44, 4031 (2019).
2. Roskill Information Services Ltd., *Titanium Minerals: Global Industry, Markets and Outlook to 2025* (London, 2016).
3. G. Zhang, K. Chou, and H. Zhao, *ISIJ Int.* 52, 1986. (2012).
4. E. Park and O. Ostrovski, *ISIJ Int.* 44, 999. (2004).
5. J. Dang, G.H. Zhang, and K.C. Chou, *J. Alloys Compd.* 619, 443. (2015).
6. W. Zhang, Z. Zhu, and C.Y. Cheng, *Hydrometallurgy* 108, 177. (2011).
7. A. Zhang, B.J. Monaghan, R.J. Longbottom, M. Nusheh, and C.W. Bumby, *Metall. Mater. Trans. B* 51, 492. (2020).
8. M.H. Bai, H. Long, S.B. Ren, D. Liu, and C.F. Zhao, *ISIJ Int.* 58, 1034. (2018).
9. I.P. Jain, *Int. J. Hydrogen Energy* 34, 7368. (2009).
10. X. Si, X. Lu, C. Li, C. Li, and W. Ding, *Int. J. Miner. Metall. Mater.* 19, 384. (2012).
11. S. Lobo, L. Kolbeinsen, and S. Seim, *Can. Metall. Q.* 55, 455. (2016).
12. G. Zhang and O. Ostrovski, *Metall. Mater. Trans. B* 31, 129. (2000).
13. G. Zhang and O. Ostrovski, *Can. Metall. Q.* 40, 317. (2001).
14. G. Zhang and O. Ostrovski, *Can. Metall. Q.* 40, 489. (2001).
15. Y. Wang, Z. Yuan, H. Matsuura, and F. Tsukihashi, *ISIJ Int.* 49, 164. (2009).
16. C.Y. Lu, X.L. Zou, X.G. Lu, X.L. Xie, K. Zheng, W. Xiao, H. Cheng, and G.S. Li, *Trans. Nonferrous Met. Soc. China* 26, 3266. (2016).
17. Z. Wang, J. Zhang, K. Jiao, Z. Liu, and M. Barati, *J. Alloys Compd.* 729, 874. (2017).
18. H.P. Gou, G.H. Zhang, and K.C. Chou, *ISIJ Int.* 55, 928. (2015).
19. Y. Zhang, J. Zhao, X. Ma, M. Li, Y. Lv, and X. Gao, *Min. Metall. Explor.* 36, 825. (2019).
20. G. Zhang and O. Ostrovski, *Int. J. Miner. Process.* 64, 201. (2002).
21. S.K. Gupta, V. Rajakumar, and P. Grieveson, *Metall. Trans. B* 22, 711. (1991).
22. S.K. Gupta, V. Rajakumar, and P. Grieveson, *Can. Metall. Q.* 28, 331. (1989).
23. X. Fu, Y. Wang, and F. Wei, *Metall. Mater. Trans. A* 41, 1338. (2010).
24. J. Zhang, Q. Zhu, Z. Xie, C. Lei, and H. Li, *Metall. Mater. Trans. B* 44, 897. (2013).
25. J. Zhang, G. Zhang, Q. Zhu, C. Lei, Z. Xie, and H. Li, *Metall. Mater. Trans. B* 45, 914. (2014).
26. S. Vyazovkin, A.K. Burnham, J.M. Criado, L.A. Pérez-Maqueda, C. Popescu, and N. Sbirrazzuoli, *Thermochim. Acta* 520, 1. (2011).
27. S. Vyazovkin and C.A. Wight, *Int. Rev. Phys. Chem.* 17, 407. (1998).